W4–W12 *Nucleic Acids Research, 2022, Vol. 50, Web Server issue* *Published online 25 May 2022*
https://doi.org/10.1093/nar/gkac396

3DGenBench: a web-server to benchmark computational models for 3D Genomics

International Nucleome Consortium[*,†]

Received March 31, 2022; Revised April 26, 2022; Editorial Decision May 03, 2022; Accepted May 23, 2022

ABSTRACT

Modeling 3D genome organisation has been booming in the last years thanks to the availability of experimental datasets of genomic contacts. However, the field is currently missing the standardisation of methods and metrics to compare predictions and experiments. We present 3DGenBench, a web server available at https://inc-cost.eu/benchmarking/, that allows benchmarking computational models of 3D Genomics. The benchmark is performed using a manually curated dataset of 39 capture Hi-C profiles in wild type and genome-edited mouse cells, and five genome-wide Hi-C profiles in human, mouse, and *Drosophila* cells. 3DGenBench performs two kinds of analysis, each supplied with a specific scoring module that compares predictions of a computational method to experimental data using several metrics. With 3DGenBench, the user obtains model performance scores, allowing an unbiased comparison with other models. 3DGenBench aims to become a reference web server to test new 3D genomics models and is conceived as an evolving platform where new types of analysis will be implemented in the future.

GRAPHICAL ABSTRACT

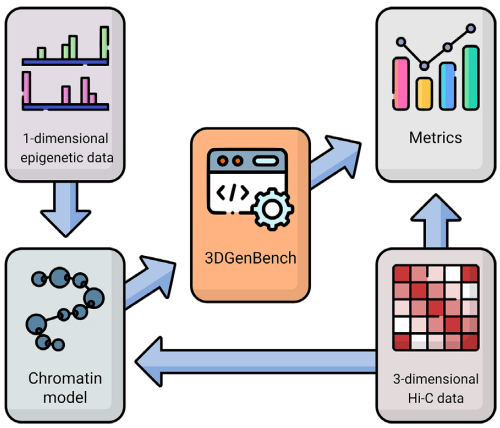

INTRODUCTION

Understanding the mechanisms driving chromatin folding is among the most challenging questions in modern genomics. Robust experimental techniques allow nowadays to obtain various datasets describing chromosome organisation and dynamics quantitatively. The plethora of genome-wide experimental data provides opportunities to infer relationships between 1D (epi)genomic and 3D genome folding properties, as well as the underlying molecular mechanisms, using statistical analysis (1,2) or biophysical modelling (3,4).

Statistical methods are being actively developed, and besides exploration of interdependencies between genomic datasets, dozens of recent models allow predictions of chromatin architecture in unseen cell types, species, and genetic conditions. Although each study contains certain benchmarks, a direct comparison of developed models is difficult due to differences in the model's input information, statistical engine, design of validation experiments and metrics characterising the model performance.

In contrast to the statistical approaches which are agnostic to the mechanisms underlying the observed dependencies, biophysical models can be used to (in)validate specific biological mechanisms or reconstruct 3D genome structures from data (3,5,6). In particular, biophysical models

[*]To whom correspondence should be addressed. Tel: +7 952 900 8413; Email: minja-f@ya.ru.
Correspondence may also be addressed to Daniel Jost. Tel: +33 4 72 72 86 30; Email: daniel.jost@ens-lyon.fr.
[†]Full authors list (see also Appendix): Polina Belokopytova, Emil Viesná, Mateusz Chiliński, Yifeng Qi, Hossein Salari, Marco Di Stefano, Andrea Esposito, Mattia Conte, Andrea M. Chiariello, Vladimir B. Teif, Dariusz Plewczynski, Bin Zhang, Daniel Jost*, Veniamin Fishman*

have predictive power and can be employed to understand the consequences of (epi)genetic perturbations (7,8) without the need to perform time-consuming and laborious experiments. However, as for statistical inference, standardised benchmarks and metrics are missing to evaluate and compare model performances and to quantify similarities between predictions and experiments.

To sum up, although multiple modeling approaches have been developed, the fundamental differences among the methodologies and validation datasets render the comparison challenging. To address this challenge, the International Nucleome Consortium (https://inc-cost.eu/) has recently started a benchmarking initiative, providing tools for the uniform assessment of computational models for 3D-Genomics. This initiative includes the collection and processing of a reference dataset based on previously published experimental data and the implementation of metrics modules scoring the similarity between experimental data and modeling results. The central component of this work is a web server, 3DGenBench, allowing users to submit their predictions and access performance metrics.

MATERIALS AND METHODS

Datasets collection

3DGenBench performs two kinds of analysis. The first type aims at quantifying how good a method predicts one experimental dataset. We defined this analysis as *horizontal* benchmarking. The second analysis, defined as *vertical* benchmarking aims to estimate how well a method can predict changes in chromosome folding caused by structural perturbations of the genome (see results text and Figure 1A for details of each analysis type). For each of these analyses, we collected specific datasets.

The data for the vertical benchmark were collected from nine studies from 2016 to 2019 (7,9–15) describing genomic mutations (deletions, inversions, duplications) of specific regions associated with chromatin architecture (Figure 1B, Supplementary Table S1). We collected and processed capture Hi-C (cHi-C) reads for wild-type (WT) and mutated conditions. Since CTCF is particularly important for chromatin architecture in vertebrates and several examples in our dataset include mutations of CTCF binding sites, we collected CTCF ChIP-seq data for relevant cell types. For this aim, we either reprocessed CTCF ChIP-seq reads obtained from the same study as cHi-C reads or, if not available, we searched for CTCF ChIP-seq experiments on matching cell type from other studies in PubMed and ENCODE datasets.

Data for the horizontal benchmarking include GM12878 and K562 human cell lines (16), mouse embryonic stem cell (mESC) line (17), and one Drosophila cell line Kc167 (18). We chose five regions for prediction for each cell type (Supplementary Table S2). Since epigenetics data are important as features for several modelling tools, we composed a table (Supplementary Table S3) with download links to the most widely used formats for several epigenetics marks for each cell type.

In addition, we used CTCF ChIA-PET dataset for human GM12878 cell line available as GEO accession GSM1872886 (19) for horizontal ChIA-PET benchmarking.

Datasets processing

Hi-C data processing. Hi-C and cHi-C data processing was performed in five steps:

1) Fetching FastQ from raw SRA datasets (fastq-dump of SRATools, NCBI);
2) Mapping reads, removing sequencing duplicates, and building fragment map (Juicer pipeline (20));
3) Building Hi-C map (JuicerTools);
4) Building COOL maps for several resolutions (5, 10, 20, 25 and 50 kb)—cooltools package (open2c) (21);
5) Hi-C map normalization—CTaleNormalize for cHi-C data (22) and cooler balance for genome-wide data.

ChIA-PET data processing. PET clusters file was downloaded from GSM1872886, single interaction for mitochondrial chromosome was removed, the remaining data were used without any further processing.

ChIP-seq data processing. All CTCF ChIP-seq data were processed using ENCODE ChIP-seq pipeline v1 (https://github.com/kundajelab/chipseq_pipeline) with parameters default for transcription factors analysis mode. Links to raw data and reference genomes are provided in Supplementary Table S1.

Performance metrics

Horizontal benchmark metrics.

- Stratum adjusted correlation coefficient (SCC) metric. SCC is a special measure to quantify the similarity between Hi-C matrices. This algorithm stratifies all Hi-C contacts according to their genomic distance and computes a Pearson correlation coefficient for each stratum. We used SCC metric (23) implemented via the *hicreppy* package (https://github.com/cmdoret/hicreppy). SCC algorithm has a tuning parameter h controlling the smoothing level. Smoothing the Hi-C matrix minimizes the effect of noise and biases. We used $h = 2$ for all comparisons.
- Insulation score (IS) metric. IS metric reflects the segmentation of the genome into domains. We used *calculate_insulation_score* function from *cooltools.api.insulation* package (version 0.5.0) with *window size* parameter equals to 5× bin size (resolution) to compute IS for all bins in the experimental and predicted data. We then computed Spearman's correlation coefficient between IS tracks obtained from experimental and predicted data.
- Compartment strength (CS) metric. CS track for experimental and predicted data was calculated as in (24). CS for each bin (b) quantifies as the ratio between the average OoE (observed over expected) value of b with bins of the same compartment and the average OoE value of b with any other bin in the same chromosome. We then used Pearson's correlation coefficient between obtained tracks as the resulting metric.

- Contacts scaling metric. We calculated the average number of contacts at separate genomic distances for experimental and predicted data. The obtained arrays of values were compared using Pearson's correlation coefficient.

ChIA-PET-specific horizontal benchmark metrics.

- The percentage of captured ChIA-PET interactions (i.e. true-positive predictions);
- The percentage of ChIA-PET interactions predicted by the model but not observed experimentally (i.e. false-positive predictions);
- The percentage of ChIA-PET observed experimentally but not predicted by the model (i.e. false-negative predictions);
- The mean-squared error of PET counts: for N overlapping PET clusters, each characterized by observed count C_i^{Exp} and predicted count C_i^{Pred}, we computed MSE as $\frac{\sum_{i\ =\ 1..N}(C_i^{Exp}-C_i^{pred})^2}{N}$

Vertical benchmark metrics.

- Insulation score changes metric. We used *calculate_insulation_score* function from *cooltools.api.insulation* package (version 0.5.0) to compute IS for all bins in the WT and mutation (Mut) conditions for experimental and predicted data. Then the Mut IS was divided by WT IS both for experimental and predicted data. Finally, we used Pearson's correlation coefficient to compare Mut/Wt experimental and Mut/Wt predicted ratio tracks.
- Ectopic interactions area under the curve (AUC) metric. Ectopic interactions for experimental and predicted data were calculated as in (7). Normalization coefficients computation accounts for the effects of the copy number changes caused by structural variants. Specifically,
  I. We normalized Mut matrix by coverage excluding contacts inside of deleted or duplicated regions. Let M be a Hi-C matrix for Mut condition with elements m_{ij}, and W be a matrix for WT condition with elements w_{ij}. Than we define normalized matrix for Mut condition as:

$$\check{M} = M * \frac{\sum_{i,j \notin del,dup} w_{ij}}{\sum_{i,j \notin del,dup} m_{ij}}$$

  In case of duplication, we computed an additional normalization coefficient as:

$$D_{coef} = \frac{\sum_{\substack{i \in dup \\ j \in dup}} w_{ij}}{\sum_{\substack{i \in dup \\ j \in dup}} \check{m}_{ij}}$$

  where $\check{m}_{ij}$ are elements of $\check{M}$.
  Next, we calculated normalized mutated matrix as:

$$\tilde{M} = \check{M} * D_{coef}$$

  where $D_{coef} = 1$ for deleted and inverted regions.
  These normalization steps were performed both for experimental and predicted data.
  II. At the second stage, we subtracted the W matrix from the $\tilde{M}$ matrix.
  III. Then we normalized the obtained differences matrix, dividing each entry by the average value at the corresponding diagonal.
  IV. Finally we calculated Z-scores at each diagonal. We filtered out elements above the 96th percentile of all diagonal values in the calculation of standard deviations.

Ectopic interactions were defined as interactions exceeding a Z-score of 2 for experimental data. These ectopic interactions for the experimental data were used as true labels for *precision_recall_curve* function from sckit-learn python library. Matrix with standard deviations of predicted data was a second argument of *precision_recall_curve* function. Different thresholds of standard deviation defined predicted ectopic interactions, precision, and recall. AUC was calculated using sckit-learn python library as well.

Generation of baselines

To provide baselines for comparison, we simulated fake predictions with varying quality either by adding different amounts of noise into experimentally observed data, or randomly by permuting observed contacts on each diagonal of a Hi-C matrix. Metrics were then computed between these baselines and the original experimental datasets.

Noise perturbation was implemented by adding a random value to each interaction of the experimental contact matrix. This random value was sampled from a normal distribution with the mean equal to the observed contact frequency and standard deviation ranging from 0.001 (the lowest noise level) to 50 (the highest noise level). We used nine control models with standard deviations equal to 0.001, 0.01, 0.01, 0.5, 1, 2, 10, 20, 50.

Diagonal shuffling was performed by grouping contacts of loci with the same genomic distance, and by randomly shuffling the observed contact values within each group. The Hi-C matrices obtained after this shuffling procedure were used as a baseline.

Generation of case study datasets

To demonstrate the metrics performance implemented in the horizontal benchmark challenge, we chose two genomic regions for GM12878 cell line at 10 Kb resolution. We used predictions generated by the DRAGON (25) and PRISMR (7) models as an example of computational predictions of chromatin architecture. DRAGON uses polymer simulations to predict Hi-C contact matrices and three-dimensional (3D) chromosome structures at five kilobase resolution from 12 key epigenetic marks and the genomic locations and orientations of CTCF binding sites. It was parameterized with a maximum entropy optimization algorithm using Hi-C data from GM12878 cells. PRISMR modelling was performed at 10 kb resolution as described before (7,26). In brief, PRISMR infers, through a recursive procedure based on polymer physics, the minimal polymer model that, at equilibrium, best describes the input contact matrix.

The inferred set of binding sites of the model correlates with key epigenetic factors and defines a code linking epigenetics to architecture, as detailed in (26). By using this code, the contact matrices of entire chromosomes can be predicted from only epigenetics (26).

To demonstrate the metrics performance for the vertical benchmark, we simulated predictions of WT and Mut data for three rearrangements (structural variants ids according to the Supplementary Table S1: deletion *MusDel-B*, inversion *Inv1*, and duplication *dup-C*) using 3DPredictor (27) and 3DPolyS-Fit (28). 3DPolyS-Fit infers pair-wise interaction strengths of a self-interacting polymer model from WT data and then use them to predict the MUT data by simulating the corresponding structural rearrangement as in (29).

Web site development

The web site was developed with the following tools:

- PureCSS (https://github.com/pure-css/pure/) style library;
- Tabulator (https://github.com/olifolkerd/tabulator) for table rendering;
- Google Charts (https://developers.google.com/chart) for plotting;

Visualization was performed with HiGlass JS API (30).

RESULTS

Benchmarking datasets and challenges

We implemented two types of analysis in the 3DGenBench benchmark platform, which we defined as *horizontal* and *vertical* benchmarking (Figure 1A). The horizontal benchmarking challenge aims at quantifying the predictive power of computational models that predict Hi-C data from locus-specific 1D-epigenetic data. For this challenge, we chose four high-resolution Hi-C datasets describing well-studied human, mouse, and *Drosophila* cell lines (human K562 and GM12868; mouse embryonic stem cells; *Drosophila* Kc167 cells). In addition, we selected CTCF ChIA-PET data for human GM12868 cells to allow scoring ChIA-PET data prediction.

To standardise the 1D-epigenetic information, we provided a list of available epigenetic tracks for each of the cell lines included in the benchmarking, such as ChIP-seq profiles, transcriptome data, and other genomic features. We limited the challenge to six 20-Mb long regions from different chromosomes, which should allow most of the models to participate in the benchmarking. Model parameters can be learned from whole genome data from which the benchmarking validation datasets are excluded. The submission to the platform consists of one predicted Hi-C map for one of the six regions of the benchmarking dataset. ChIA-PET data submission consists of a single file of PET clusters.

We implemented several metrics measuring model performance in the horizontal benchmarking challenge (see Materials and Methods). For Hi-C data, these included Spearman's correlation and stratum adjusted correlation coefficient (SCC) (23) to measure overall similarity of experimental and predicted Hi-C maps. SCC is advantageous over correlation because it is not biased by the strong distance dependence of chromatin interaction data. We measured the accuracy of the predicted distance dependence separately as the correlation between observed and predicted contact scaling functions. We used Pearson's correlation between predicted and observed compartmentalization profiles (24) to show how well the model captures preferences in interactions between chromatin compartments. Finally, we used Spearman's correlation of insulation scores to estimate how the model predicts boundaries of topologically associating domains (TADs). Since there are multiple models predicting TAD boundaries without inferring contact maps, we provided an option to submit insulation scores tracks only. To support visual assessment of the predicted data, we integrated a HiGlass view in the 3DGenBench output pages.

For ChIA-PET data prediction the overlap between predicted and reference lists of PET clusters are estimated (see Materials and Methods) and the mean-squared error of

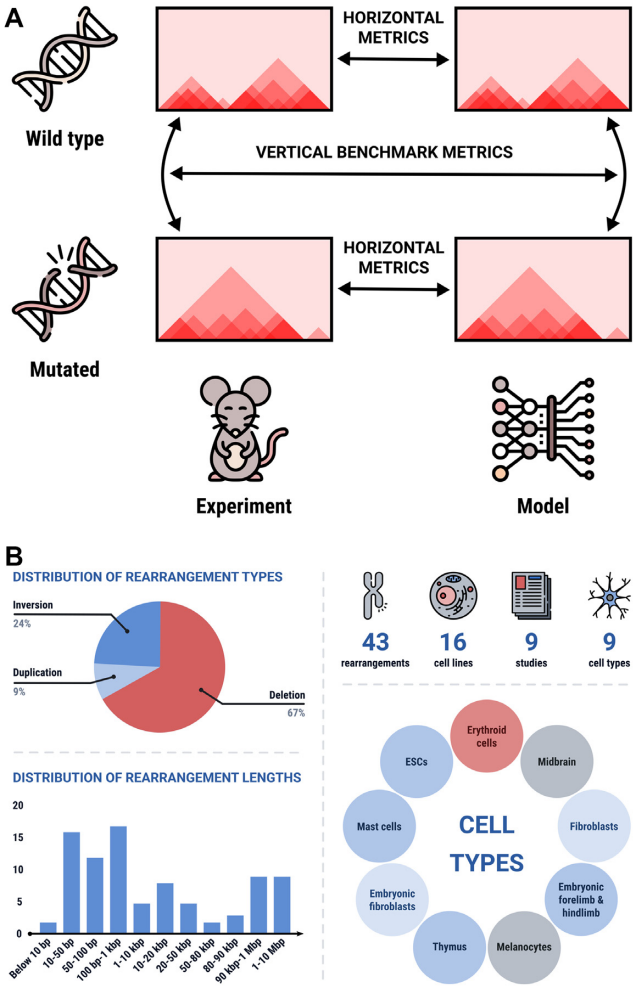

Figure 1. Benchmarking analysis provided by 3DGenBench. (**A**) Horizontal benchmarking consists of comparing experimental data and model in the same condition (i.e. WT versus WT or Mut versus Mut). Vertical benchmarking aims to quantify the accuracy of the model in predicting changes of chromatin architecture due to the mutations. (**B**) Graphical summary of the datasets collected for the vertical benchmark.

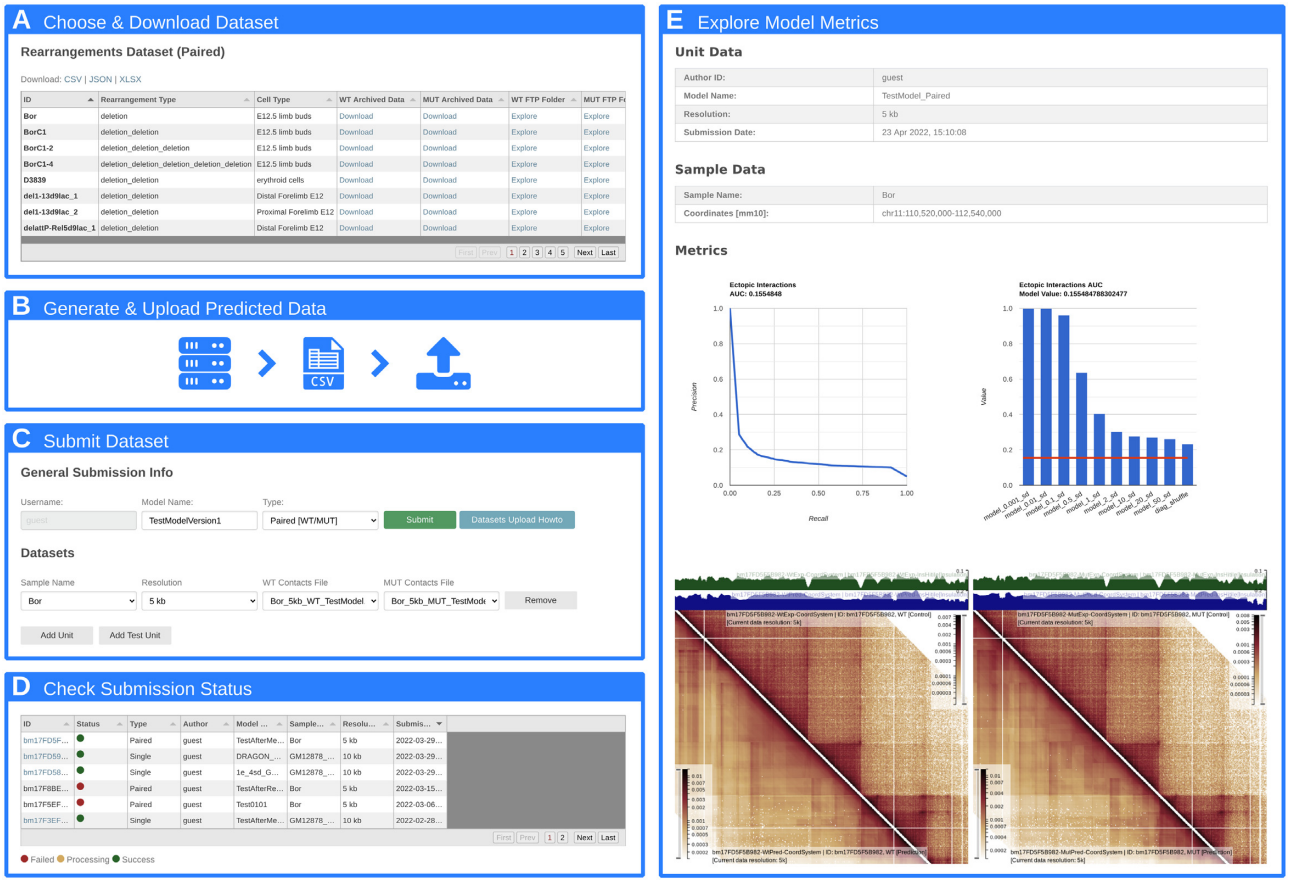

Figure 2. The main steps of the 3DGenBench workflow. (**A**) Dataset selection and download. (**B**) Generation and upload of predicted data. (**C**) Job submission. (**D**) Submission status validation. (**E**) Exploring results.

PET counts is computed to estimate the accuracy of cluster counts.

The second type of analysis implemented in the 3DGenBench platform is called *vertical* challenge. It aims at quantifying how accurate models are in predicting *changes* of chromatin architecture caused by genetic perturbations. For this challenge, we collected capture Hi-C-datasets available for CRISPR-edited mouse cells and tissues with matched wild-type controls. The resulting dataset includes 49 wild-type—mutation pairs from nine loci and nine cell types (Figure 1B). The input data for this type of analysis consists of a pair of predicted Hi-C datasets matching experimental wild-type and mutation data. For each wild-type—mutation pair, 3DGenBench will extract the fraction of chromatin interactions that differ between both conditions. 3DGenBench then compares this predicted set of ectopic interactions with experimentally observed differences.

We implemented several previously-published metrics, specifically measuring how the model captures differences in chromatin architecture between two conditions (see Materials and Methods). These metrics score the overlap between observed and predicted ectopic chromatin interactions (7) and predictions of TAD boundaries changes.

3DGenBench workflow, input and output description

We expect the following usage of the 3DGenBench services. First, modellers can explore the 3DGenBench datasets available under the '*Datasets*' tab to find relevant experimental data for benchmarking (Figure 2A). Each Hi-C dataset is available in the most commonly used formats: hic, cool (5, 10, 20 and 50 kb resolutions), and pairs. Also, there are supplementary tracks describing CTCF binding sites for most of the datasets. All the data can be downloaded via hyperlinks in the table. Alternatively, the complete metadata table can be obtained from the server in JSON or text format to fetch and process download URLs automatically.

After exploring and modeling experimental data, predictions for the corresponding datasets can be uploaded to the server via FTP or the submission page (Figure 2B). Predicted Hi-C contacts should be formatted as 4-column files, each row containing the chromosome name, two genomic coordinates, and contact count (see Supplementary Data 1 for a representative example); ChIA-PET predictions as 6-column files, with the same format as the pairs format utilized by 4DNucleome portal (https://www.4dnucleome.org/). Example files are available at the 3DGenBench tutorial pages. Users can upload multiple files that will appear in the drop-down list at the next (submission) step.

Once the data is uploaded, users can follow the 'Compute metrics' tab from the home menu, choose the type of prediction (single for horizontal benchmarking or paired for vertical benchmarking) and fill all the fields related to the predicted sample (Figure 2C).

The status of the submission is then available at the 'Submissions list' tab of the home menu (Figure 2D). Blue status

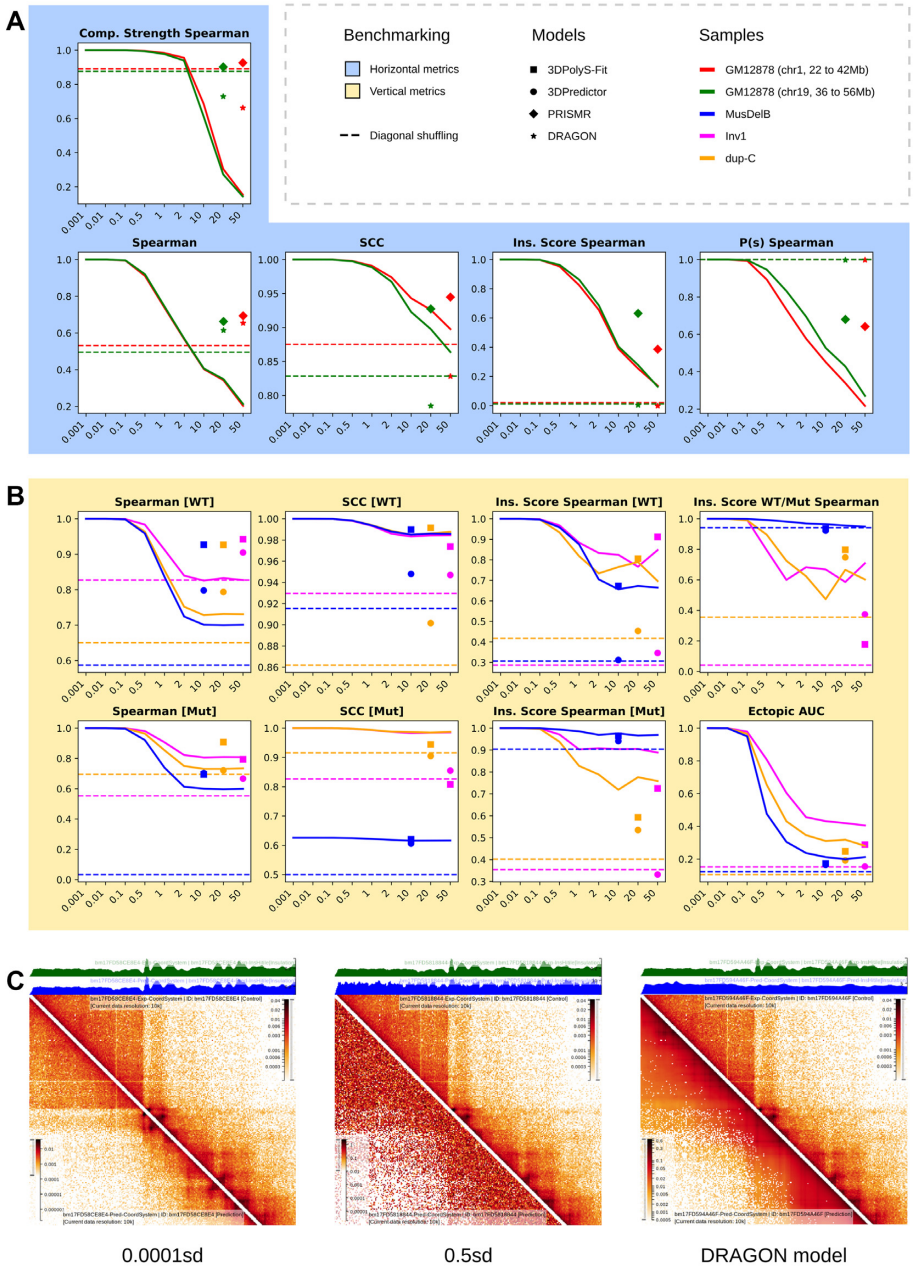

Figure 3. Examples of scoring metrics provided by 3DGenBench. (**A**) Example of vertical benchmarking using 3DGenBench. Performance metrics comparing experimental Hi-C data with noise-injected datasets (solid lines), diagonal shuffling (dashed horizontal lines), DRAGON (asterisk) and PRISMR (diamond) models. Data is shown for two loci of GM12878 cells on chromosome 1 (orange) and chromosome 19 (blue). X-axes show noise levels (measured in standard deviation values, the higher the value the noisier the data, see Materials and Methods for details). Y-axes show corresponding metric values. (**B**) Example of vertical benchmark. Data is presented as in (A). (**C**) HiGlass views comparing experimental data (above diagonal) with two noise-injected datasets and DRAGON model (below diagonal) for genomic region 22–42 Mb on chromosome 1 in GM12878 cells.

of submission indicates that the job is queued; yellow status of submission indicates the server is currently being processed the job; green status means that metrics computation was successfully completed, and red indicates an error with data processing.

When data processing is over, clicking on the ID link (e.g. bmXXXXXXXX) redirects the user to the page with the job results (Figure 2E). This page contains metrics describing the prediction accuracy of the model. In addition, the result pages shows metrics obtained for baselines, simulating predictions of varying quality (see Materials and Methods for details). It is also possible to compare with previously-submitted jobs by choosing any available IDs with a green colour of the status icon.

Case study

To evaluate how 3DGenBench scores the similarity between Hi-C datasets, we generated fake predictions by injecting different amounts of noise into experimental Hi-C

data or by randomly shuffling contacts on each diagonal of Hi-C matrices (see Materials and Methods) and submitted all generated datasets to the 3DGenBench platform. We also generated predictions for contact maps of two loci in GM12878 cells based on 1D epigenomic data (horizontal challenge) using the DRAGON and PRISMR chromatin models (7,25,26), and predicted three pairs of WT and Mut contact maps (vertical challenge) using 3DPredictor, and 3DPolyS-Fit algorithms (25,27,28).

As shown in Figure 3A for horizontal benchmarking, the 3DGenBench metrics are concordant with the level of noise injection. Noisier models have lower SCC, compartmentalization and insulation score similarity metrics. Interestingly, metrics show differ sensitivity to noise injections. The correlation coefficient computed from all contacts decreases even when a small amount of noise was added to contacts, whereas compartments strength and insulation scores were relatively stable at these noise levels. Diagonal shuffling expectedly preserve contacts scaling, but result in strong changes of the insulator score.

According to our metrics, the DRAGON model perfectly captures contact scaling, shows good metrics of compartment prediction, but is less efficient regarding the insulation landscape (Figure 3A and C). PRISMR model captures insulation landscape significantly better than DRAGON model, but is not as good in predicting contacts scaling. This toy example shows how 3DGenBench can be used to discover strengths and weaknesses of different predictive models.

Similarly, 3DGenBench correctly scores noise injection models in vertical benchmarking (Figure 3B). For example, precision-recall AUC gradually decreases from 1 to ∼0.2 when increasing the amount of noise. Our comparison of 3DPredictor and 3DPolyS-Fit algorithms shows that in most of cases 3DPolyS-Fit reconstructs chromatin architecture and its changes better than 3DPredictor, although in few cases (i.e. for prediction of insulation score changes in the inversion Inv1) 3DPredictor outperforms 3DPolyS-Fit. Overall, this shows that the 3DGenBench metrics module provides a user-friendly interface to score computational predictions of genome architecture.

CONCLUSIONS AND FUTURE PROSPECTS

Here, we describe 3DGenBench, a web-platform for benchmarking of computational models of 3D chromatin architecture. There are two types of analysis implemented in 3DGenBench currently, but this platform can be easily extended to include additional species, cell types and benchmarks. It can be used by model developers to improve their methods based on robust metrics but also by model users to choose the best methods to tackle their questions. One promising direction of 3DGenBench development is the integration with 4DNucleome datasets (31), which is currently the largest available collection of 3D genomic data. In addition, different types of data could be integrated, e.g. from microscopy based experimental approaches (32), to test the models at the single molecule level (33) beyond the population averaged contact maps. Another future direction is the development of online services implementing the most popular algorithms for chromatin modelling. Currently, the vast majority of computational models do not have user-friendly implementations, and only few of them have online-tools allowing simple access (27,34). A web-implementation of these modeling tools alongside with benchmarking results provided by 3DGenBench platform will allow the 4D Genomics community to easily integrate chromatin models in their research.

DATA AVAILABILITY

The 3DGenBench web server is accessible at https://inc-cost.eu/benchmarking/. The corresponding open-source code is available in the GitHub repository (https://github.com/regnveig/3DGenBench).

SUPPLEMENTARY DATA

Supplementary Data are available at NAR Online.

ACKNOWLEDGEMENTS

We thank all the members of the 'International Nucleome Consortium' COST action for fruitful discussions and support.

FUNDING

International Nucleome Consortium is supported by COST (European Cooperation in Science and Technology) [CA18127]; analysis of Hi-C data by V.F. and P.S.B. were supported by the RSF project [21-65-00017]; 3DGenBench web-site development was supported by IT-facilities of the Institute of Cytology and Genetics Project [121031800061-7] (mechanisms of genetic control of development, physiological processes and behavior in animals); ChIP-seq data collection and analysis was supported by grant [2019-0546] (FSUS-2020–0040); M.C. and D.P. were supported by National Science Centre, Poland [2019/35/O/ST6/02484]; research in the Jost lab (H.S., D.J.) is supported by Agence Nationale de la Recherche [ANR-18-CE45-0022-01]; Y.Q. and B.Z. acknowledge support from the National Institutes of Health [R35GM133580]. Funding for open access charge: COST Action INC [CA18127], supported by COST (European Cooperation in Science and Technology).
Conflict of interest statement. None declared.

REFERENCES

1. Tao,H., Li,H., Xu,K., Hong,H., Jiang,S., Du,G., Wang,J., Sun,Y., Huang,X., Ding,Y. *et al.* (2021) Computational methods for the prediction of chromatin interaction and organization using sequence and epigenomic profiles. *Brief. Bioinform.*, **22**, bbaa405.
2. Belokopytova,P. and Fishman,V. (2021) Predicting genome architecture: challenges and solutions. *Front. Genet.*, **11**, 1–15.
3. Di Stefano,M., Paulsen,J., Jost,D. and Marti-Renom,M.A. (2021) 4D nucleome modeling. *Curr. Opin. Genet. Dev.*, **67**, 25–32.
4. Oluwadare,O., Highsmith,M. and Cheng,J. (2019) An overview of methods for reconstructing 3-D chromosome and genome structures from Hi-C data. *Biol. Proced. Online*, **21**, 7.
5. Mirny,L.A., Imakaev,M. and Abdennur,N. (2019) Two major mechanisms of chromosome organization. *Curr. Opin. Cell Biol.*, **58**, 142–152.

6. Bianco,S., Chiariello,A.M., Conte,M., Esposito,A., Fiorillo,L., Musella,F. and Nicodemi,M. (2020) Computational approaches from polymer physics to investigate chromatin folding. *Curr. Opin. Cell Biol.*, **64**, 10–17.
7. Bianco,S., Lupiáñez,D.G., Chiariello,A.M., Annunziatella,C., Kraft,K., Schöpflin,R., Wittler,L., Andrey,G., Vingron,M., Pombo,A. *et al.* (2018) Polymer physics predicts the effects of structural variants on chromatin architecture. *Nat. Genet.*, **50**, 662–667.
8. Qi,Y., Reyes,A., Johnstone,S.E., Aryee,M.J., Bernstein,B.E. and Zhang,B. (2020) Data-Driven polymer model for mechanistic exploration of diploid genome organization. *Biophys. J.*, **119**, 1905–1916.
9. Barutcu,A.R., Maass,P.G., Lewandowski,J.P., Weiner,C.L. and Rinn,J.L. (2018) A TAD boundary is preserved upon deletion of the CTCF-rich firre locus. *Nat. Commun.*, **9**, 1444.
10. Franke,M., Ibrahim,D.M., Andrey,G., Schwarzer,W., Heinrich,V., Schöpflin,R., Kraft,K., Kempfer,R., Jerković,I., Chan,W.-L. *et al.* (2016) Formation of new chromatin domains determines pathogenicity of genomic duplications. *Nature*, **538**, 265–269.
11. Hanssen,L.L.P., Kassouf,M.T., Oudelaar,A.M., Biggs,D., Preece,C., Downes,D.J., Gosden,M., Sharpe,J.A., Sloane-Stanley,J.A., Hughes,J.R. *et al.* (2017) Tissue-specific CTCF-cohesin-mediated chromatin architecture delimits enhancer interactions and function in vivo. *Nat. Cell Biol.*, **19**, 952–961.
12. Kraft,K., Magg,A., Heinrich,V., Riemenschneider,C., Schöpflin,R., Markowski,J., Ibrahim,D.M., Acuna-Hidalgo,R., Despang,A., Andrey,G. *et al.* (2019) Serial genomic inversions induce tissue-specific architectural stripes, gene misexpression and congenital malformations. *Nat. Cell Biol.*, **21**, 305–310.
13. Kragesteen,B.K., Spielmann,M., Paliou,C., Heinrich,V., Schöpflin,R., Esposito,A., Annunziatella,C., Bianco,S., Chiariello,A.M., Jerković,I. *et al.* (2018) Dynamic 3D chromatin architecture contributes to enhancer specificity and limb morphogenesis. *Nat. Genet.*, **50**, 1463–1473.
14. Paliou,C., Guckelberger,P., Schöpflin,R., Heinrich,V., Esposito,A., Chiariello,A.M., Bianco,S., Annunziatella,C., Helmuth,J., Haas,S. *et al.* (2019) Preformed chromatin topology assists transcriptional robustness of shh during limb development. *Proc. Natl. Acad. Sci. U.S.A.*, **116**, 12390–12399.
15. Rodríguez-Carballo,E., Lopez-Delisle,L., Zhan,Y., Fabre,P.J., Beccari,L., El-Idrissi,I., Huynh,T.H.N., Ozadam,H., Dekker,J. and Duboule,D. (2017) The HoxD cluster is a dynamic and resilient TAD boundary controlling the segregation of antagonistic regulatory landscapes. *Genes Dev.*, **31**, 2264–2281.
16. Rao,S.S.P., Huntley,M.H., Durand,N.C., Stamenova,E.K., Bochkov,I.D., Robinson,J.T., Sanborn,A.L., Machol,I., Omer,A.D., Lander,E.S. *et al.* (2014) A 3D map of the human genome at kilobase resolution reveals principles of chromatin looping. *Cell*, **159**, 1665–1680.
17. Bonev,B., Mendelson Cohen,N., Szabo,Q., Fritsch,L., Papadopoulos,G.L., Lubling,Y., Xu,X., Lv,X., Hugnot,J.-P., Tanay,A. *et al.* (2017) Multiscale 3D genome rewiring during mouse neural development. *Cell*, **171**, 557–572.
18. Cubeñas-Potts,C., Rowley,M.J., Lyu,X., Li,G., Lei,E.P. and Corces,V.G. (2017) Different enhancer classes in drosophila bind distinct architectural proteins and mediate unique chromatin interactions and 3D architecture. *Nucleic Acids Res.*, **45**, 1714–1730.
19. Tang,Z., Luo,O.J., Li,X., Zheng,M., Zhu,J.J., Szalaj,P., Trzaskoma,P., Magalska,A., Wlodarczyk,J., Ruszczycki,B. *et al.* (2015) CTCF-mediated human 3D genome architecture reveals chromatin topology for transcription. *Cell*, **163**, 1611–1627.
20. Durand,N.C., Shamim,M.S., Machol,I., Rao,S.S.P., Huntley,M.H., Lander,E.S. and Aiden,E.L. (2016) Juicer provides a one-click system for analyzing loop-resolution Hi-C experiments. *Cell Syst.*, **3**, 95–98.
21. Venev,S., Abdennur,N., Goloborodko,A., Flyamer,I., Fudenberg,G., Nuebler,J., Galitsyna,A., Akgol,B., Abraham,S., Kerpedjiev,P. *et al.* (2021) Open2c/cooltools: v0.4.1 Zenodo. https://zenodo.org/record/5214125#.YoeUt1RByUk.
22. Golov,A.K., Ulianov,S.V., Luzhin,A.V., Kalabusheva,E.P., Kantidze,O.L., Flyamer,I.M., Razin,S.V. and Gavrilov,A.A. (2020) C-TALE, a new cost-effective method for targeted enrichment of Hi-C/3C-seq libraries. *Methods*, **170**, 48–60.
23. Yang,T., Zhang,F., Yardımcı,G.G., Song,F., Hardison,R.C., Noble,W.S., Yue,F. and Li,Q. (2017) HiCRep: assessing the reproducibility of Hi-C data using a stratum-adjusted correlation coefficient. *Genome Res.*, **27**, 1939–1949.
24. Falk,M., Feodorova,Y., Naumova,N., Imakaev,M., Lajoie,B.R., Leonhardt,H., Joffe,B., Dekker,J., Fudenberg,G., Solovei,I. *et al.* (2019) Heterochromatin drives compartmentalization of inverted and conventional nuclei. *Nature*, **570**, 395–399.
25. Qi,Y. and Zhang,B. (2019) Predicting three-dimensional genome organization with chromatin states. *PLoS Comput. Biol.*, **15**, e1007024.
26. Esposito,A., Bianco,S., Chiariello,A.M., Abraham,A., Fiorillo,L., Conte,M., Campanile,R. and Nicodemi,M. (2022) Polymer physics reveals a combinatorial code linking 3D chromatin architecture to 1D chromatin states. *Cell Rep.*, **38**, 110601.
27. Belokopytova,P.S., Nuriddinov,M.A., Mozheiko,E.A., Fishman,D. and Fishman,V. (2020) Quantitative prediction of enhancer-promoter interactions. *Genome Res.*, **30**, 72–84.
28. Szabo,Q., Jost,D., Chang,J.-M., Cattoni,D.I., Papadopoulos,G.L., Bonev,B., Sexton,T., Gurgo,J., Jacquier,C., Nollmann,M. *et al.* (2018) TADs are 3D structural units of higher-order chromosome organization in drosophila. *Sci. Adv.*, **4**, eaar8082.
29. Giorgetti,L., Galupa,R., Nora,E.P., Piolot,T., Lam,F., Dekker,J., Tiana,G. and Heard,E. (2014) Predictive polymer modeling reveals coupled fluctuations in chromosome conformation and transcription. *Cell*, **157**, 950–963.
30. Kerpedjiev,P., Abdennur,N., Lekschas,F., McCallum,C., Dinkla,K., Strobelt,H., Luber,J.M., Ouellette,S.B., Azhir,A., Kumar,N. *et al.* (2018) HiGlass: web-based visual exploration and analysis of genome interaction maps. *Genome Biol.*, **19**, 125.
31. Dekker,J., Belmont,A.S., Guttman,M., Leshyk,V.O., Lis,J.T., Lomvardas,S., Mirny,L.A., O'Shea,C.C., Park,P.J., Ren,B. *et al.* (2017) The 4D nucleome project. *Nature*, **549**, 219–226.
32. Bintu,B., Mateo,L.J., Su,J.-H., Sinnott-Armstrong,N.A., Parker,M., Kinrot,S., Yamaya,K., Boettiger,A.N. and Zhuang,X. (2018) Super-resolution chromatin tracing reveals domains and cooperative interactions in single cells. *Science*, **362**, eaau1783.
33. Conte,M., Fiorillo,L., Bianco,S., Chiariello,A.M., Esposito,A. and Nicodemi,M. (2020) Polymer physics indicates chromatin folding variability across single-cells results from state degeneracy in phase separation. *Nat. Commun.*, **11**, 3289.
34. Wlasnowolski,M., Sadowski,M., Czarnota,T., Jodkowska,K., Szalaj,P., Tang,Z., Ruan,Y. and Plewczynski,D. (2020) 3D-GNOME 2.0: a three-dimensional genome modeling engine for predicting structural variation-driven alterations of chromatin spatial structure in the human genome. *Nucleic Acids Res.*, **48**, W170–W176.

APPENDIX

[+]Full authors list:
Polina Belokopytova[1,2,3], Emil Viesná[1,3], Mateusz Chiliński[4,5], Yifeng Qi[6], Hossein Salari[7], Marco Di Stefano[8], Andrea Esposito[10], Mattia Conte[10], Andrea M. Chiariello[10], Vladimir B. Teif[9], Dariusz Plewczynski[4,5], Bin Zhang[6], Daniel Jost[7,*] and Veniamin Fishman[1,2,3,11*]

1 Institute of Cytology and Genetics, Novosibirsk 630090, Russia
2 Research Institute of Medical Genetics, Tomsk National Research Medical Center of the Russian Academy of Sciences, Tomsk 634009, Russia
3 Novosibirsk State University, Novosibirsk 630090, Russia
4 Laboratory of Bioinformatics and Computational Genomics, Faculty of Mathematics and Information Science, Warsaw University of Technology, Koszykowa 75, 00-662 Warsaw, Poland

5 Laboratory of Functional and Structural Genomics, Centre of New Technologies, University of Warsaw, Banacha 2c, 02-097 Warsaw, Poland
6 Department of Chemistry, Massachusetts Institute of Technology, Cambridge, MA, USA
7 Laboratoire de Biologie et Modelisation de la Cellule, Ecole Normale Superieure de Lyon, CNRS, UMR 5239, Inserm, U1293, Universite Claude Bernard Lyon 1, 46 allee d'Italie F-69364 Lyon, France
8 Institute of Human Genetics, University of Montpellier, CNRS, Laboratoire de Chromatine et Biologie Cellulaire, Montpellier, France
9 School of Life Sciences, University of Essex, Wivenhoe Park, Colchester CO4 3SQ, UK
10 Dipartimento di Fisica, Universita' degli Studi di Napoli Federico II, and INFN Napoli, Complesso Universitario di Monte Sant'Angelo, 80126 Naples, Italy
11 Artificial Intelligence Research Institute, AIRI, Moskow, Russia